Gallium concentration effects on the properties of $CuIn_{1-x}Ga_xSe_2$ ingots

S. GAGUI[a*], B. HADJOUDJA[a], B. CHOUIAL[a], B. ZAIDI[a], Y. KOUHLANE[a], N. BENSLIM[b], A. CHIBANI[a]

[a]*Laboratory of Semiconductors, Department of physics, University Badji Mokhtar, Annaba, Algeria*
[b]*Laboratory of Study of Surfaces and Interfaces of Solid Matter, Department of physics,*
University Badji Mokhtar, Annaba, Algeria

In this paper, we report on the crystal growth of $CuIn_{1-x}Ga_xSe_2$ ingots with different gallium concentrations ($0 \leq x \leq 1$), and investigate the influence of these concentrations on the structural, optical and electrical properties of these compounds. The preferred orientation in the (112) direction was obtained, and the main XRD peaks showed a noticeable shift to higher diffraction angles with increasing Ga content. The lattice parameters "a" and "c" have been calculated from the X-ray spectra and were found to decrease with the increase of gallium concentration. In addition the c/a ratio was found to be close to 2. The band gap E_g increased when the Ga/(In+Ga) ratios increased. The ingots have p-type conductivity and their resistivity varied between 6.41 and 32.64 Ωcm with a minimum value of 0.67 Ωcm for x=0.4.

1. Introduction

$CuIn_{1-x}Ga_xSe_2$ (CIGS) compounds are the most promising materials for thin films solar cells fabrication [1-7]. They possess a high absorption coefficient (10^5 cm^{-1}) in the visible spectrum, a tunable band gap width ranging from 1.0 eV for $CuInSe_2$ to 1.7 eV for $CuGaSe_2$ [8, 9]. This tunability is achieved by just varying the parameter x=Ga/(In+Ga) [10]. These advantages have made it possible for the solar cells based on the CIGS materials to reach a record value 20.8 % [11]. Balboul et al. [12] have found that the best efficiency CIGS solar cells was obtained for the lattice parameter ratio c/a≈2. Different methods have been used to prepare bulk $CuIn_{1-x}Ga_xSe_2$ ($0 \leq x \leq 1$) absorbers such the Bridgman technique [13-15], the gradient freezing method [16], the travelling heater method (THM) [17] and a novel melting method for CIGS [18]. In this work, we have chosen a technique similar to that of Djellal et al. [15], in order to investigate the effect of gallium on the structural, optical and electrical properties of $CuIn_{1-x}Ga_xSe_2$ ingots.

2. Experimental details

$CuIn_{1-x}Ga_xSe_2$ ingots with different compositions x=Ga/(In+Ga) = 0; 0.2; 0.4; 0.6; 0.8 and 1 have been prepared by direct melting method. The elemental materials of 99.999 % purity were weighted for obtaining a stoichiometric mixture which is introduced in quartz ampoule which was subsequently evacuated to 10^{-6} Torr, sealed and then placed in a furnace where the mixture was subjected to an optimized thermal cycle. The thermal treatment is constituted of six different stages: heating from ambient temperature up to 300 °C at 1 °C/min, where

this temperature is maintained for 5 hours after which a second heating stage at 1 °C/min raises the temperature to 1150 °C where it is kept at that level for 24 h. During this fusion stage the quartz ampoule was rotated continuously to ensure homogeneity in the molten mixture. Then the crystallization process is initiated by a first cooling stage at 1 °C/min from the melt dawn to 950 °C where this level is maintained for 24 h. A second cooling at 1 °C/min lowers the temperature down to the ambient and thus terminates he synthesis process.

The structural properties of the obtained ingots were determined by X-ray diffraction (XRD) using a PANalytical X'pert PRO Instrument diffractometer with Cu Kα (λ= 1.54056 Å) radiation, over the 2θ range 10–90° with a step size of 0.02°. A scanning electron microscope (SEM), associated with an energy dispersive spectrometer (EDS) were used respectively to examine the morphology of ingots and to determine the chemical composition of their constituents. Absorption measurements were carried out at room temperature using a Cary 5000 UV-Vis-NIR spectrophotometer at a scanning rate of 200 nm/min in the wavelength range 280-1200 nm. The electrical properties (resistivity, mobility, conductivity) were also determined at room temperature by an HMS 3000 Hall Effect measurement system.

3. Results and discussion

3.1. Morphology and chemical composition

The chemical composition of constituents is obtained after analysis of five different parts of the ingot $CuIn_{1-x}Ga_xSe_2$. The results given in Table 1 show that the

compositions of all samples were slightly copper rich. Similar results have been reported by other authors [19].

The properties of Cu(In,Ga)Se$_2$ films are affected by the chemical composition, especially the ratio of Cu/(In+Ga). Lundberg et al. [10] have showed that the best solar cells efficiency were obtained for the ratio Cu/(In+Ga) comprised between 0.9 and 1. On the other hand, Li et al. [20] have shown that the Cu-rich films were converted to Cu-poor films by the annealing process.

Table 1. Chemical composition of the CuIn$_{1-x}$Ga$_x$Se$_2$ with different composition x.

Samples	Cu(at %)	In(at %)	Ga(at %)	Se(at %)	Cu/(In+ Ga)
CuInSe$_2$	27.18	24.28		48.54	1.11
CuIn$_{0.8}$Ga$_{0.2}$Se$_2$	25.83	19.98	4.72	49.47	1.04
CuIn$_{0.6}$Ga$_{0.4}$Se$_2$	26.77	14.55	9.42	49.26	1.11
CuIn$_{0.4}$Ga$_{0.6}$Se$_2$	24.72	9.95	14.40	50.93	1.01
CuIn$_{0.2}$Ga$_{0.8}$Se$_2$	29.67	4.67	19.01	46.65	1.25
CuGaSe$_2$	24.56		23.70	51.74	1.03

The scanning electron microscope (SEM) images of CuIn$_{0.6}$Ga$_{0.4}$Se$_2$, CuIn$_{0.4}$Ga$_{0.6}$Se$_2$ samples are shown in Fig. 1. We notice the good crystalinity of the CuIn$_{0.6}$Ga$_{0.4}$Se$_2$ sample in comparison with CuIn$_{0.4}$Ga$_{0.6}$Se$_2$. This is probably due to the defects concentration which increases when the proportion of gallium increases.
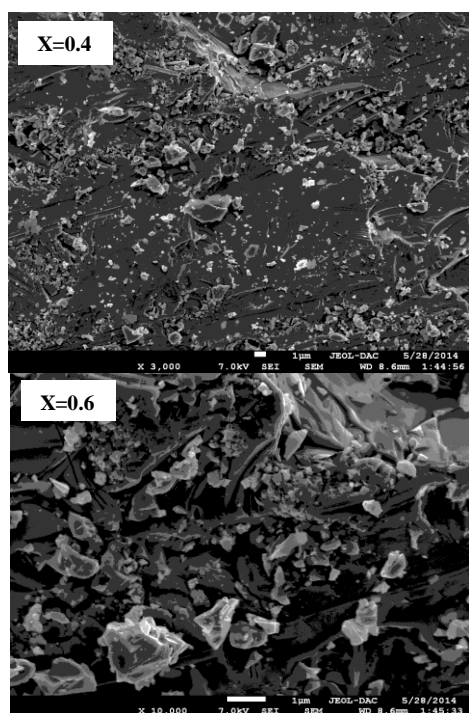

Fig. 1. SEM images of CuIn$_{1-x}$Ga$_x$Se$_2$ ingots for x=0.4 and 0.6.

3.2. Structural properties

The X-ray diffraction patterns of CuIn$_{1-x}$Ga$_x$Se$_2$ ingots with different compositions are shown in Fig. 2. The results show that single-phase CIGS samples were prepared. These spectra show that the orientation planes (112), (220/204) and (312/116) have a high intensity with a preferential orientation according to the direction (112). All the observed positions of the peak corresponding to (112) orientation are found to shift linearly to higher values of 2θ with the increase in gallium proportion as illustrated in Fig. 3. This noticeable shift is attributed to Ga atoms substituting for In atoms in the chalcopyrite structure. This behavior has been reported in the literature [21, 22]. Note that the ingots with Ga/(In+Ga) ≤ 0.6 exhibited single XRD peaks for the (220/204), (116/312) and (332/316). However when Ga portion increases, this doublet peaks, are observed to be split into two individual peaks (220)/(204), (116)/(312) and (332)/(316). The split of doublet peak indicates a deviation of tetragonality, induced by Ga substitution. Indeed this behavior was observed by other authors [22, 23]. The presence of the peaks related to (400)/(008) direction implies that gallium takes partly the place of indium in the tetragonal CIS phase and then results in the tetragonal CIGS phase. This result has been reported in the literature [12, 23]. Furthermore the presence of the peaks (112), (220)/(204), (116)/(312), (400) and (332) which appear more clearly for the quaternary CuIn$_{0.6}$Ga$_{0.4}$Se$_2$ confirm the chalcopyrite structure of our samples.

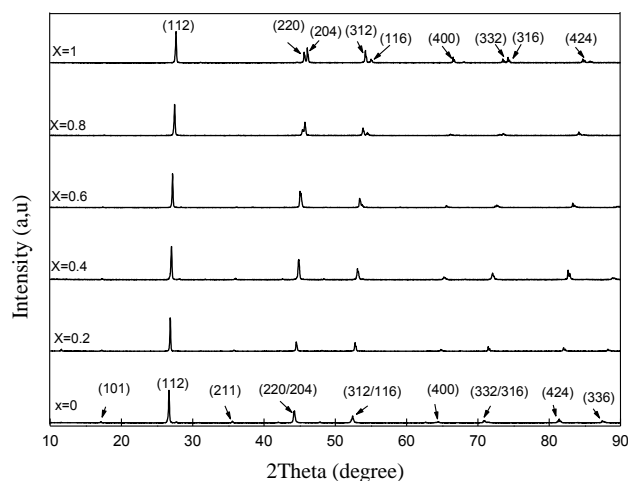*Fig. 2. XRD patterns of the CuIn$_{1-x}$Ga$_x$Se$_2$ bulk with different x.*

The full width at half maximum (FWHM) of (112) peaks of the CIGS ingots were calculated. Fig. 4 shows the variation of the FWHM function the composition x of the prepared CIGS.

FWHM is found to be nearly constant as the gallium concentration increases. This result has been reported by other authors [22, 24]. The grain size in the ingots has been obtained from the calculation using the main X-ray

diffraction peak broadening by the well-known Scherrer formula:

$$d= 0.9\lambda/(B_r \cos\theta)$$

Where λ is the wavelength of Cu-ka radiation (λ = 0.154 nm), and B_r is the full-width at half-maximum (FWHM) of the main peak and θ is the main peak position. Figure 5 shows that the crystalline sizes are in the range between 592 and 692 Å. Similar result have been reported by other authors [19, 25].
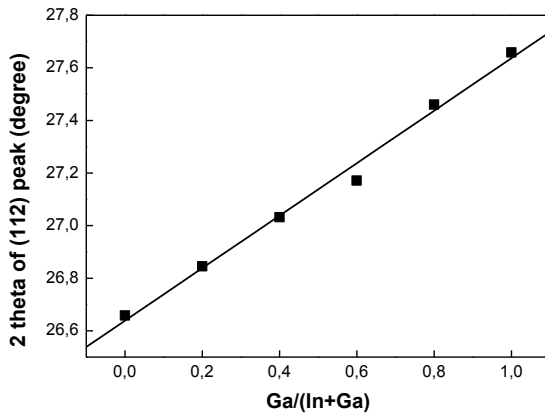

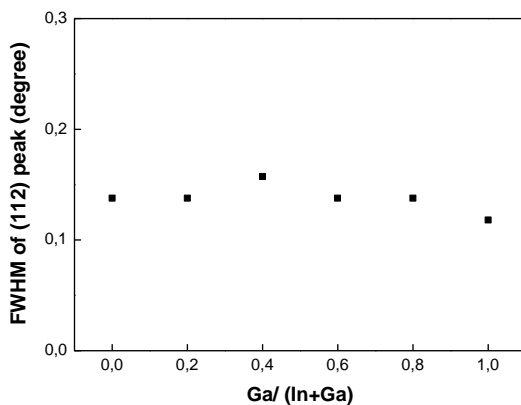*Fig. 3. Shift of the (112) peak position as a function of the Ga/(In+Ga) ratios.*

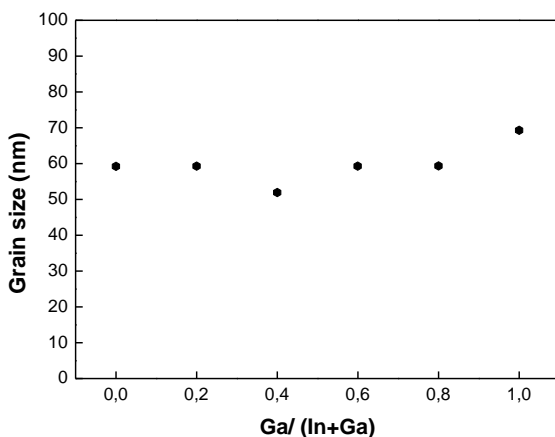*Fig.4. Variation of FWHM as a function of Ga/(In+Ga) ratio.*

Fig. 5. Variation of grain size as a function of Ga/(In+Ga) ratio.

The lattice parameters "a" and "c" were calculated from the X-ray spectra. Their variation and that of c/a are shown in Fig. 6. The lattice parameters are found to decrease with the increasing of Ga/(In +Ga) ratio. This is due to the small ionic size of Gallium (0.62 Å) compared to that of indium (0.81 Å) and hence causes a shrinkage of the lattice as they substitute indium sites in the network. These results are in good agreement with those obtained by other authors [12, 26]. The c/a ratio calculated from the lattice parameters "a" and "c" was found to be close to 2. Moreover, the variation of lattice constants with Ga/(ln+Ga) ratio in $GuIn_{1-x}Ga_xSe_2$ bulk could be fitted to : a(x)= 5.791 - 0.168 x and c(x) = 11.600 – 0.554 x.

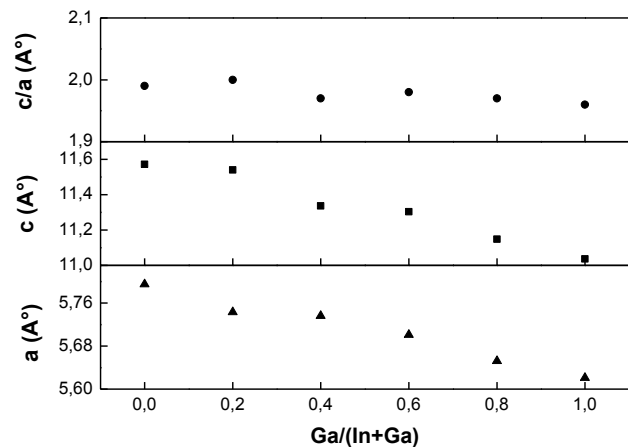*Fig. 6. Lattice parameters "a", "c" and c/a in the function of the Ga/(In+Ga) ratio.*

3.3 Optical properties

Fig. 7 shows the plots of $(\alpha h v)^2$ versus the photon energy hv and the optical absorption spectra of different concentration of gallium. From this characteristic, $(\alpha h v)^2$ versus hv, we seek to determine the value of the gap energy of the investigated compound. The gap energy is determined by taking the tangent to the curve for the low energies, or by extrapolating the linear region to the intersection with the abscissa axis. When $(\alpha h v)^2$ is zero, the photon energy is E_g. The variation of the band gap (E_g) as a function of Ga/(In+Ga) ratios are shown in Fig. 8. The obtained optical band gap values varied from 1.05 eV to 1.65 eV when the Ga content increased from 0 to 1. Band gap E_g increased with the increase of composition x. A similar type of variation was observed [10, 20, 26].

The variation of E_g with Ga/(In+Ga) ratios can be fitted to a parabolic (polynomial Fit), and is expressed by the following relationship:

$$E_g(x) [eV] = 1.03536 + 0.48768 x + 0.12946 x^2$$

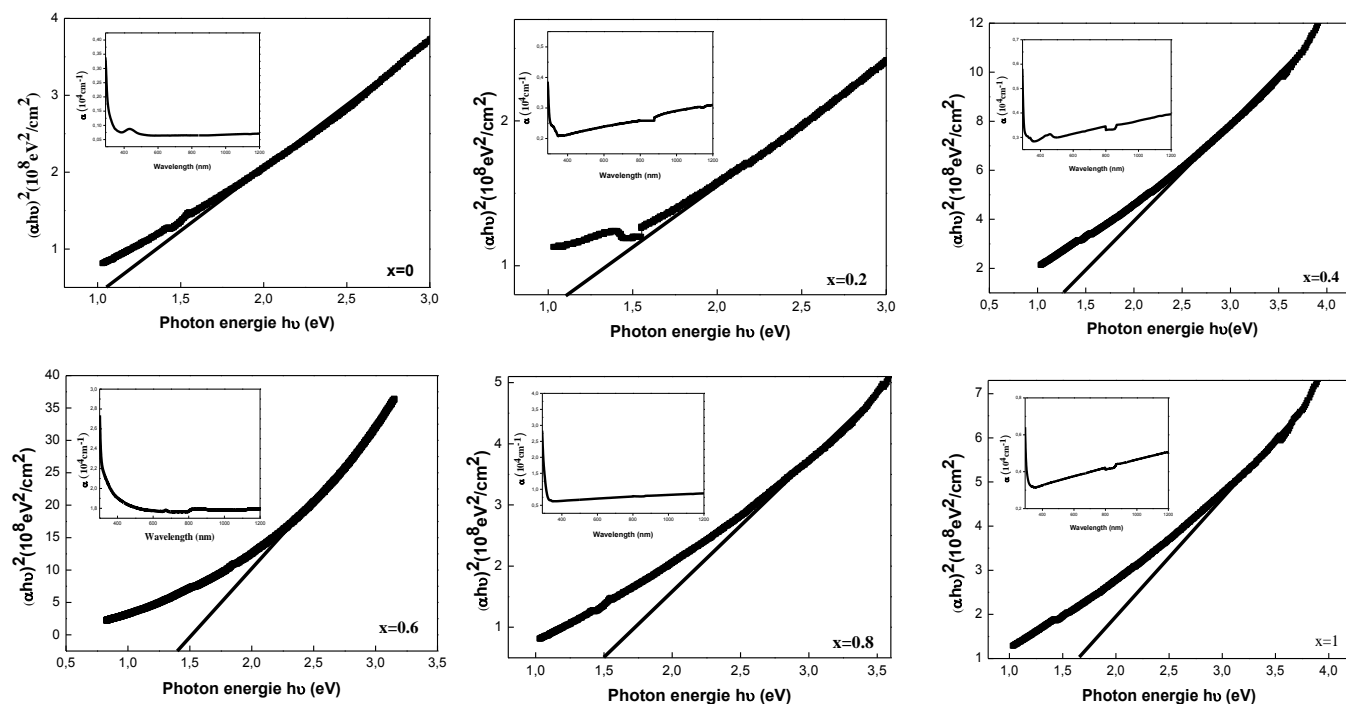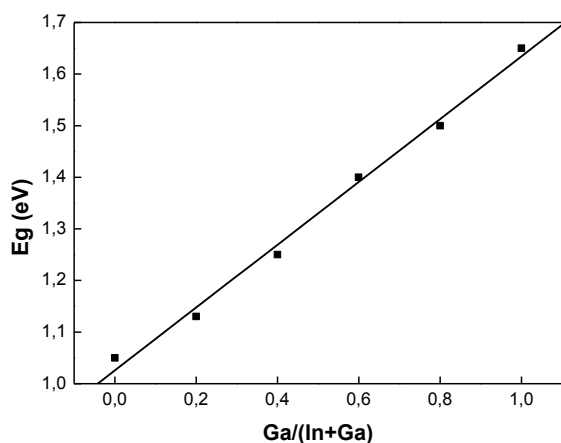*Fig. 7. Plots of (αhv)^2 versus photon energy hv of CuIn$_{1-x}$Ga$_x$Se$_2$ ingots.*

Fig. 8. Variation of energy gap as a function Ga/(In+Ga) ratio.

3.4. Electrical properties

The ingots were found to have a p-type conductivity and their resistivity varied between 6.41 and 32.64 Ωcm with a minimum value of 0.67 Ωcm for x=0.4 as illustrated in Fig. 9. This value is lower by one order of magnitude than those obtained by other authors [27, 28]. The carriers concentration was found to vary between 2.10^{15} and 6.10^{16} cm^{-3} with a maximum of 5.10^{17} cm^{-3} for x=0.4. Fig. 10 shows the variation of the conductivity as a function of the band gap width of the CuIn$_{1-x}$Ga$_x$Se$_2$ compounds.

The best conductivity is obtained for a gap close to 1.25 eV, corresponding to a gallium proportion x=0.4.

Kwon et al. [29] have shown the best gallium proportion for solar cells fabrication is x=0.35. On the other hand, Contreras et al. [30] have show that a gallium proportion greater 0.35 permits to obtain solar cells having an acceptable performance.
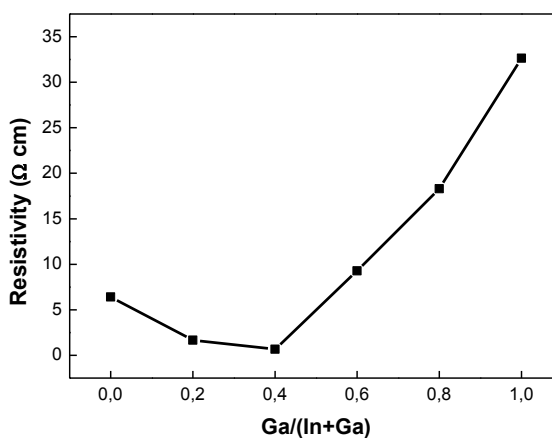

Fig. 9. Variation of resistivity as a function Ga/(In+Ga) ratio.

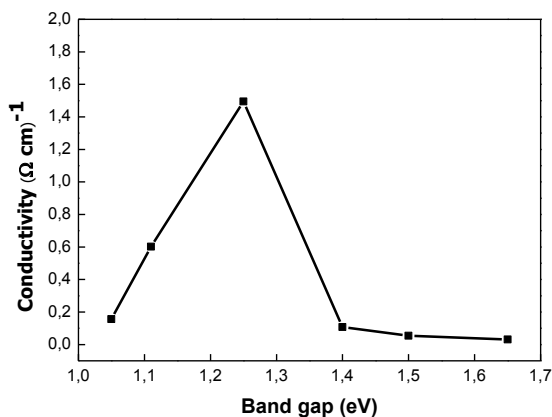*Fig. 10. Variation of conductivity as a function of band gap width of $CuIn_{1-x}Ga_xSe_2$ ingots.*

4. Conclusion

We synthesized $CuIn_{1-x}Ga_xSe_2$ ingots by direct melting method with gallium content $0 \leq x \leq 1$.

The structure, composition, morphology, optical and electrical properties of the prepared ingots were investigated. The preferential orientation in the (112) direction was obtained, and the main XRD peaks showed a noticeable shift to higher diffraction angles with increasing Ga content. The lattice parameters "a" and "c" have been calculated from the X-ray spectra and both of them were found to decrease with increasing of gallium concentration. In addition the c/a ratio was found to be close to 2 and the presence of the peaks (112), (220)/(204), (116)/(312), (400) and (332) indicate that the prepared ingots are of chalcopyrite structure. The band gap E_g increased when the Ga/(In+Ga) ratios increased. The band gap E_g=1.25 eV was obtained for x=0.4. All the ingots have p-type conductivity and their resistivity varied between 6.41 and 32.64 Ωcm with a minimum value of 0.67 Ωcm for x=0.4. These obtained results indicate that the prepared $CuIn_{0.6}Ga_{0.4}Se_2$ ingot has the prerequisite properties required by the solar cells absorber layers.

References

[1] Z. Yu, Y. Yan, S. Li, Y. Zhang, C. Yan, L. Liu, Y. Zhang, Y. Zhao, Appl. Surf. Sci. **264,** 197 (2013).

[2] H. J. Jo, D. H. Jeon, B. S. Ko, S. J. Sung, D. K. Hwang, J. K. Kang and D. H. Kim, Curr. Appl. Phys., **14**, 318 (2014).

[3] W. L. Wang, H. Lin, J. Zhang, X. Li, A. Yamada, M. Konagai and J. B. Li, Sol. Energy Mater. Sol. Cells, **94**, 1753 (2010).

[4] N. Barreau, J. Lähnemann, F. Couzinié-Devy, L. Assmann, P. Bertoncini and J .Kessler, Sol. Energy Mater. Sol. Cells, **93**, 2013 (2009).

[5] H. M. Friedlmeier, P. M. Pérez, I. Klugius, P. Jackson, O. Kiowski, E. Ahlswede M. Powalla, Thin Solid Films, **535**, 92 (2013).

[6] V. S. Saji, I. H. Choi, C. W. Lee, Sol. Energy, **85**, 2666 (2011).

[7] D. Nam, S. Jung, S. Ahn, J. Gwak, K. Yoon, J. H. Yun, H. Cheong, Thin Solid Films, **535**, 118 (2013).

[8] Z. Han, D. Zhang, Q. Chen, R. Hong, C. Tao, Y. Huang, Z. Ni and S. Zhuang, Mater. Res. Bull., **51**, 302 (2014).

[9] C J. Stolle, T. B. Harvey and B. A. Korgel, Curr. Opinion in Chem. Eng., **2**, 160 (2013).

[10] O. Lundberg, M. Edoff and L. Stolt, Thin Solid Films, **480–481**, 520 (2005).

[11] P. Jackson, D. Hariskos, R. Wuerz, W. Wischmann M. Powalla, Physica status solidi (RRL) - Rapid Research Letters, **8**, 219 (2014).

[12] M. R. Balboul, H. W. Schock, S. A. Fayak, A. Abdel El-Aal, J. H. Werner and A. A. Ramadan, Appl. Phys. A, **92**, 557 (2008).

[13] W. S. Weng, L. S. Yip, I. Shih, C. H. Champness, Revue canadienne de phys., **67**, 294 (1989).

[14] M. Lachab, A. A. Attia and C. Llinarès, J. Cryst. Growth, **280,** 474 (2005).

[15] L. Djellal, A. Bouguelia, M. Kadi Hanifi, M. Trari, Sol. Energy Mater. Sol. Cells, **92**, 594 (2008).

[16] M. A. Arsene, A. Albacete, F. Voillot, J. P. Peyrade, A. Barra, J. Galibert, S. M. Wasim, E. Hernandez, J. Cryst. Growth, **158**, 97 (1996).

[17] H. Miyake, K. Sugiyama, J. Cryst. Growth, **125**, 548 (1992).

[18] T. Chen, Y. Zhao, Z. Dong, J. Yang, T. Liu, Mater. Letters, **106,** 52 (2013).

[19] M. Venkatachalam, M. D. Kannan, S. Jayakumar, R. Balasundaraprabhu and N. Muthukumarasamy, Thin Solid Films, **516**, 6848 (2008).

[20] Z. H. Li, E. S. Cho and S. J. Kwon, Curr. Appl. Phys., **11,** 28 (2011).

[21] B. Vidhya, S. Velumani, A. Jesus, A. Alatorre, A. Morales-Acevedo, R. Asomoza, J. A. Chavez-Carvayar, Mater. Sci. & Eng., **174**, 216 (2010).

[22] D. Y. Lee, S. J. Park and J. H. Kim, Curr. Appl. Phys., **11**, S88 (2011).

[23] S. Jung, S. J. Ahn, J. H. Yun, J. Gwak, D. Kim, K. Yoon, Curr. Appl. Phys., **10**, 990 (2010).

[24] S. Y. Kim, J. H. Kim, Korean Phys. Soc. **6**, 2018 (2012).

[25] M. Venkatachalam, M. D. Kannan, S. Jayakumar, R. Balasundaraprabhu, A. K. Nandakumar, N. Muthukumarasamy, Sol. Energy Mater. Sol. Cells, **92**, 571 (2008).

[26] B. A. Mansour, I. K. El Zawawi and H. Shaban, J. of mater. Sci. : mater. in electron., , **14**, 63 (2003).

[27] L. Zhang, Q. He, W. L. Jiang, C. J. Li, Y. Sun, Chin. Phys. Lett., **26**, 026801(2009).

[28] L. Zhang, Q. He, H. L. Jiang, F. F. Liu, C. J. Li, Y. Sun, Sol. Energ. Mater. Sol. Cells **93**, 114 (2009).

[29] S. H. Kwon, D. Y. Lee, B. T. Ahn, J. of the Korean Phys. Soc., , **39**, 655 (2001).

[30] M. A. Contreras, H. Wiesner, J. Tuttle, K. Ramanathan, R. Noufi, Sol. Energy Mater. Sol. Cells, **49**, 239 (1997).

_____
*Corresponding author: souheyla_gagui@yahoo.fr